ELF/VLF wave generation from the beating of two HF ionospheric heating sources

M. B. Cohen,[1] R. C. Moore,[2] M. Golkowski,[3] and N. G. Lehtinen[1]

Received 19 July 2012; revised 28 September 2012; accepted 24 October 2012; published 13 December 2012.

[1] It is well established that Extremely Low Frequency (ELF, 0.3–3 kHz) and Very Low Frequency (VLF, 3–30 kHz) radio waves can be generated via modulated High Frequency (HF, 3–10 MHz) heating of the lower ionosphere (60–100 km). The ionospheric absorption of HF power modifies the conductivity of the lower ionosphere, which in the presence of natural currents such as the auroral electrojet, creates an 'antenna in the sky.' We utilize a theoretical model of the HF to ELF/VLF conversion and the ELF/VLF propagation, and calculate the amplitudes of the generated ELF/VLF waves when two HF heating waves, separated by the ELF/VLF frequency, are transmitted from two adjacent locations. The resulting ELF/VLF radiation pattern exhibits a strong directional dependence (as much as 15 dB) that depends on the physical spacing of the two HF sources. This beat wave source can produce signals 10–20 dB stronger than those generated using amplitude modulation, particularly for frequencies greater than 5–10 kHz. We evaluate recent suggestions that beating two HF waves generates ELF/VLF waves in the *F*-region (>150 km), and conclude that those experimental results may have misinterpreted, and can be explained strictly by the much more well established D region mechanism.

Citation: Cohen, M. B., R. C. Moore, M. Golkowski, and N. G. Lehtinen (2012), ELF/VLF wave generation from the beating of two HF ionospheric heating sources, *J. Geophys. Res.*, *117*, A12310, doi:10.1029/2012JA018140.

1. Introduction

[2] Extremely Low Frequency (ELF, 0.3–3 kHz) and Very Low Frequency (VLF, 3–30 kHz) radio waves are difficult to generate with conventional antennas, due primarily to their long wavelengths (10–1000 km). On the other hand, ELF/VLF waves have broad applications to ionospheric and magnetospheric remote sensing, and long distance communications. A practically realizable and permanent vertical antenna is much shorter than a wavelength and thus can radiate reasonable ELF/VLF power only after being tuned to a narrow frequency band [*Watt*, 1967]. On the other hand, the ELF/VLF radiation from a horizontal antenna will suffer from the image current just beneath the conducting ground which cancels out the power radiated by the antenna.

[3] Recent decades have seen new research into creating an 'antenna in the sky', to overcome the limitations of practical ELF/VLF transmitter design. The first observations by *Getmantsev et al.* [1974] in the USSR were followed by a long series of experiments at Tromsø Norway [*Stubbe et al.*, 1981; *Barr and Stubbe*, 1984; *Rietveld et al.*, 1984, 1987; *Barr et al.*, 1987; *Barr and Stubbe*, 1991, 1997; *Barr*, 1998], and later at the High Frequency Active Auroral Research Program (HAARP) facility near Gakona, Alaska, which was upgraded in 2007 to 3.6 MW of power [*Cohen et al.*, 2008a; *Golkowski et al.*, 2008, 2011; *Cohen et al.*, 2011; *Moore and Agrawal*, 2011; *Fujimaru and Moore*, 2011]. Using a High Frequency (HF, 3–30 MHz) transmitter on the ground, the free ionospheric electrons in the lower ionosphere are heated, thus changing the conductivity of the ionosphere. The lower ionosphere as defined here includes 60–100 km altitude, and is referred to here as the *D* region although it also includes the lowest part of the *E* region (85–100 km). In the presence of natural currents such as the auroral electrojet, periodic modulation of the HF heating imposes the same modulation on the electrojet currents, thus radiating the modulation frequency (as well as at its harmonics). HF heaters have been built in Russia, Norway, Alaska, and Puerto Rico, and consist of a grid of antennas capable of focusing HF energy into a narrow upward beam, with effective radiated powers as high as the GW range.

[4] Although the generated signals have been detected as far as 4400 km away [*Moore et al.*, 2007; *Cohen et al.*, 2010c], two key limitations of this scheme remain before it could possibly be used as a practical communications system: (1) the efficiency remains quite low, on the order of ~0.001% [*Moore et al.*, 2007], and (2) the generation mechanism requires the presence of natural ionospheric currents, greatly constraining the feasible locations and

[1]Department of Electrical Engineering, Stanford University, Stanford, California, USA.
[2]Department of Electrical Engineering, University of Florida, Gainesville, Florida, USA.
[3]Department of Electrical Engineering, University of Colorado Denver, Denver, Colorado, USA.

Corresponding author: M. B. Cohen, Department of Electrical Engineering, Stanford University, 350 Serra Mall, Rm. 356, Stanford, CA 94305, USA. (mcohen@stanford.edu)

0148-0227/12/2012JA018140

limiting the reliability (an equatorial electrojet HF heating facility has not yet been constructed, although a powerful VHF radar at Jicamarca, Peru, did generate a weak 2.5 kHz signal when modulated [*Lunnen et al.*, 1984]). The first limitation has been mitigated by a recent advance that utilizes beam steering rather than square wave amplitude modulation that delivers ~10 dB more ELF/VLF power than vertical AM heating [*Cohen et al.*, 2008b, 2010b], although further increases in efficiency are needed. Recent suggestions to use dual beam ionospheric heating [*Moore and Agrawal*, 2011] and time of arrival analysis [*Fujimaru and Moore*, 2011] may lead to additional efficiency improvements.

[5] One proposed technique to circumvent the need for an electrojet is to attempt to generate waves in the *F* region. Presently, at least two approaches to *F* region generation have been investigated experimentally. *Papadopoulos et al.* [2011] described driving pressure gradients in the *F* region to form magneto-sonic waves, which then convert to Hall currents in the *E* region. The second proposed method involves broadcasting two continuous HF waves from the ground separated by a ELF/VLF frequency [*Kuo et al.*, 2011, 2012]. We discuss here the second of these two methods.

[6] A prominent pioneering work on the beating of two HF sources for wave generation is that of *Barr and Stubbe* [1997], using the Tromsø heating facility. The six rows of an antenna grid were divided into two halves, each with three rows. One half was driven with a continuous 4.04 MHz input, and the other with a frequency higher by the desired ELF/VLF generation frequency. Hardware limitations prevented a large frequency separation, but for the two frequencies tested (565 Hz and 2006 Hz), the signals observed 500 km to the south were substantially weaker (11 dB) from the beat wave technique compared to the a square wave technique in which the HF power is keyed on and off. However, *Barr and Stubbe* [1997] then describe a simplified model of the wave generation (assuming a *D* region source), which matched experimental results, and then used the theory to predict that the beat wave approach would produce higher amplitudes on the ground at higher frequencies than they were able to test. *Villaseñor et al.* [1996] also compare a beat wave approach (referred to therein as DF) with amplitude modulation using the High-Power Auroral Stimulation (HIPAS) facility in Alaska, and present evidence for a common source height based on wave polarizations as a function of frequency, and confirm that the DF technique can produce stronger amplitudes above 5 kHz.

[7] *Kuo et al.* [2011] describe a physical process by which the same beat wave technique could produce a source of waves in the *F*-region via an electrojet-independent mechanism, under proper geomagnetic conditions (low *D* region absorption) and choice of HF frequency. Using the HAARP facility, *Kuo et al.* [2011] cite a case where magnetometer activity was weak, and yet generation of ELF/VLF waves via beat wave was observed to occur. Recent work by *Jin et al.* [2011], however, shows that a weak magnetometer reading does not imply that there will be no generation. *Kuo et al.* [2012] then provided a comparison between the beat wave and amplitude modulation techniques, showing that the former can be stronger. On the other hand, *Moore et al.* [2012] used an observational time of arrival technique in conjunction with a beat wave experiment to show that the source region was in the *D* region, not the *F* region.

[8] In this work, we evaluate theoretically the generation of ELF/VLF waves via beat waves from two closely spaced (i.e., on the order of wavelengths) HF sources heating the *D* region, and find substantial enhancement of wave generation compared to sinusoidal power modulation. The resulting directional dependence is also similar to the geometric modulation techniques [*Cohen et al.*, 2008b, 2010b]. In particular, the separation of the two HF sources on the ground create a phasing effect in the *D* region of the ionosphere which changes the spatial distribution of ELF/VLF signals on the ground. We find that the experimental results of both *Kuo et al.* [2011] and *Kuo et al.* [2012] can be explained using only a *D* region source. We note that these results are consistent with the original findings presented by *Barr and Stubbe* [1997], although the model presented herein is more complete. Furthermore, we extend the conclusion to a different modulation waveform for which the voltage envelope to the antenna array is modulated as the square root of a sine wave, so that the HF power radiated is modulated sinusoidally, identical to the technique utilized by *Kuo et al.* [2012]. We will refer to this modulation as sinusoidal power modulation. It is worth noting that square wave amplitude modulation, as used by *Barr and Stubbe* [1997], typically produces 1–3 dB stronger signals than sinusoidal power modulation. onger signals).

2. Model Description

[9] We utilize a pair of three-dimensional models which together simulate the HF to ELF/VLF conversion and propagation process, described by *Cohen et al.* [2010a]. The HF heating model is based on earlier work [*Tomko*, 1981; *Rodriguez*, 1994; *Moore*, 2007; *Payne et al.*, 2007]. The model solves an energy balance equation that includes collisional heating and cooling, and assumes a Maxwellian electron energy distribution as described by page 165 of *Bittencourt* [2003].

$$\frac{3}{2}N_e k_B \frac{dT_e}{dt} = 2k\chi S - L_e(T_e, T_0) \tag{1}$$

where T_e is the heated electron temperature, N_e is the electron density, k_B is Boltzmann's constant, k is the wave number, χ is the imaginary (absorbing) part of the refractive index calculated from the Appleton-Hartree equation, S is the HF power density, and L_e is a sum of electron loss terms, each a function of T_e and the ambient electron temperature (T_0).

[10] The electron loss rates are documented by pages 175–178 of *Rodriguez* [1994], with the elastic loss rates given by *Banks* [1966], the rotational excitation loss rates given by *Mentzoni and Row* [1963] and *Dalgarno et al.* [1968], and the vibrational excitation loss rates given by *Stubbe and Varnum* [1972]. The modified electron temperature modifies the collision frequency as discussed by page 176 of *Rodriguez* [1994]. An effective collision frequency of $\frac{5}{3}\nu$, as discussed by *Sen and Wyller* [1960], is used to calculate the Hall and Pedersen conductivity according to page 137 of *Tomko* [1981], assuming a constant electrojet electric field. HF refraction and wave normal angle bending are also taken into account as described by chapter 2 of *Moore* [2007].

[11] The electron-neutral collision frequency and electron temperature are evolved in time, in a three dimensional

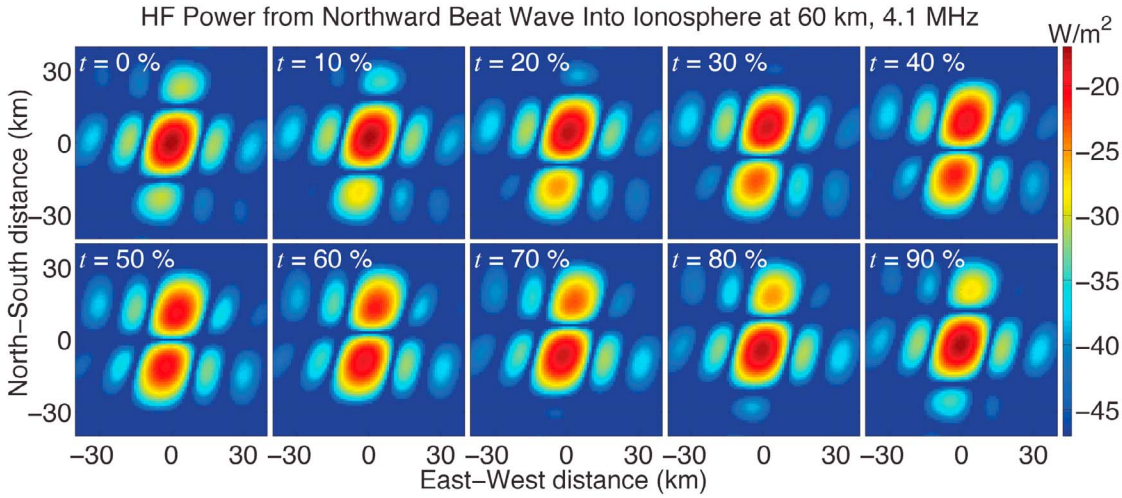

Figure 1. The HF heating pattern from the northward beat wave experiment, at 4.1 MHz, over a horizontal slice reaching 60 km altitude centered above HAARP. The pattern is shown at 10 different times in the ELF/VLF cycle, indicated by the labels in the top left corner of each panel.

space. From these, the model calculates the Hall and Pedersen ionospheric conductivity magnitudes, and extracts the amplitude and phase of the first harmonic. The ionospheric electron density is assumed based on the IRI model for a high latitude summer nighttime. The electron density is assumed to not be affected by the HF heating process, since the energy density is too low to ionize in the lower ionosphere, and the electron density changes from slower chemical changes take many minutes to take effect [*Milikh and Papadopoulos*, 2007]. The geomagnetic field is taken from the IGRF model for 2011. The field line at HAARP has declination ∼22° and dip angle ∼16°.

[12] The amplitudes and phases of the conductivity changes yield current sources, with the electrojet-induced electric field assumed to be 10 mV/m (consistent with *Cohen et al.* [2010a]). These current sources, embedded in the ionosphere and spatially distributed, are fed as input into a full wave model of ELF/VLF wave propagation [*Lehtinen and Inan*, 2008, 2009]. The propagation model yields the electric and magnetic field values in and below the ionosphere. In this paper, we focus on the predicted amplitudes received on the ground.

[13] The HF heating model takes as input the power density as a function of time in a two-dimensional slab at the bottom of the ionosphere, in this case 60 km altitude. The power density is calculated by summing the phasor contributions of the two sources assuming free space propagation. The two phasors add constructively, then destructively, alternating at the difference frequency, producing power modulation at the difference frequency at each given location. Because the spacing of the two HF sources is significant compared to a wavelength, the phase of the power modulation at each point is a strong function of space. From 60 km upward, the HF energy is then propagated through the ionosphere taking into account absorption. The time steps utilized are 1 μs, short enough that the energy balance equation can be linearized. In this case, the HF power input from HAARP is assumed to come from two HF sources, representing two halves of the array. The entire array is 12 rows, with ∼24.4 m between them, so the two half-grid sources are assumed to be 146.3 m apart, or six rows.

[14] For the amplitude modulation simulations, the voltage envelope to the antenna array is modulated as the square root of a sine wave, so that the HF power radiated is modulated sinusoidally, identical to the technique utilized by *Kuo et al.* [2012].

3. Results

[15] The realistic radiation pattern of each half-grid is taken as input into the model, based on measurements at the HAARP array, including a main lobe and a series of smaller sidelobes (at least 10 dB lower peak power density) stratified to the north, south, east, and west along the grid of the HAARP array. The two sources (one for each half of the grid) are separated by a difference frequency, and the HF power into the *D* region of the ionosphere results from the interference of these two sources as a function of time.

[16] Figure 1 shows an example of the HF power input resulting from the split-array beat-wave technique at 4.1 MHz. The spatial distribution changes periodically, at the ELF/VLF separation frequency. One may consider this situation as if the two HF sources are offset in phase by an amount that changes in time, and wraps around 360° every ELF/VLF period, and separated by 146.3 m (almost precisely two HF wavelengths at 4.1 MHz). The 10 panels show the HF power density at ten points in the ELF/VLF period, as a function of space, for an 80 km × 80 km box centered at 60 km altitude and directly above HAARP, oriented to geographic north and south. In the top left panel, at the beginning of the ELF/VLF period, the two HF sources are in phase, so that their power adds constructively directly above HAARP. The secondary power regions, 10–15 dB less in power, result from the sidelobes, which also constructively interfere between the two sources. Because the HAARP array is aligned 14° east of geographic north, the sidelobes are also oriented along an axis in this direction. The two HF sources are separated in this direction. For the rest of this paper, the term 'north' with respect to HAARP refers to

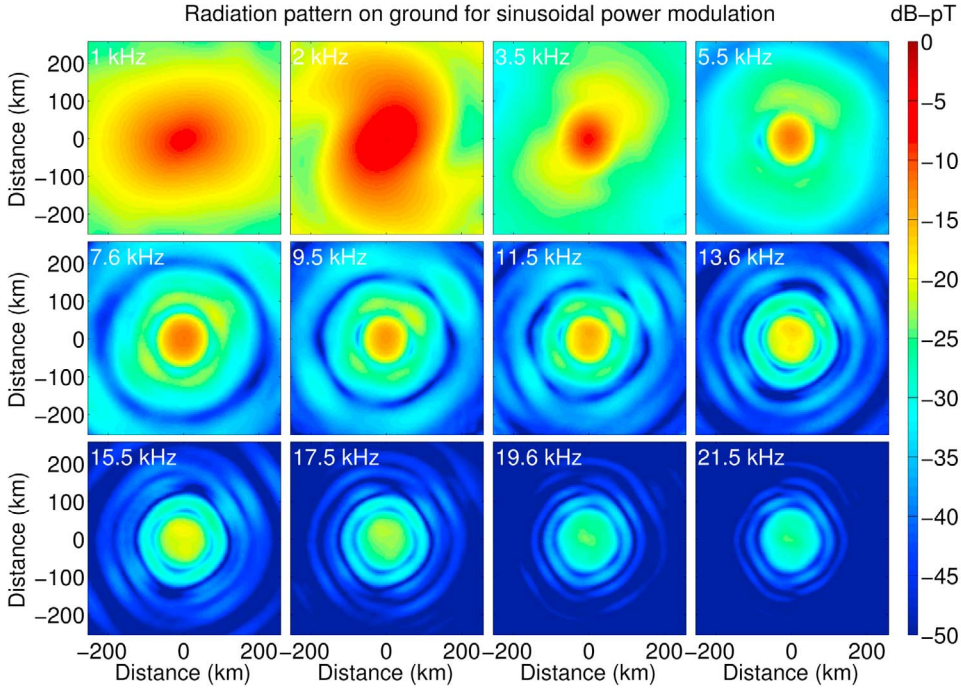

Figure 2. The calculated magnetic field amplitude on the ground (total horizontal component) for amplitude modulation with a sinusoidal power envelope. The 12 panels each reflect the a 500 km × 500 km box around HAARP, and the 12 panels represent 12 different frequencies, labeled in the top left corner of each panel.

14° east of north, or along the direction of HAARPs northward column. The ERP of HAARP at 4.1 MHz is ~1.16 GW, so that the maximum power density at 60 km altitude is ~26 mW/m^2. In these simulations, we use X-mode polarization, although the HF radiation pattern would not be different for O-mode or linear polarization.

[17] The HF beam pattern can be interpreted as exhibiting substantial motion in time, as earlier noted by *Kotik et al.* [1986], *Rapoport et al.* [1994], and *Barr and Stubbe* [1997], and in a similar manner to the 'sawtooth sweep' described by *Cohen et al.* [2008b], in which the HF power is left on continuously, and a thin beam is swept in a linear direction (then starting over from the other end), repeating every ELF/VLF period. In the case shown in Figure 1, the more northward of the two HF sources is lower in HF frequency, so that after 10% of the ELF/VLF cycle, its phase lags the southward HF source by 36°. Hence, the point of constructive interference between the two sources is shifted to the north (as are the sidelobes). As the ELF/VLF period progresses, reflected by the labels in the upper left corner of each panel, the center of the HF heating beam continues to shift northward, along with the southward sidelobe which also moves along with the main beam while gaining peak power. At the midway point, reflected in the bottom left panel, the two HF sources are 180° out of phase, resulting in destructive interference directly above HAARP. From that point, what had been the main beam begins to lose power and become a sidelobe, whereas the southward side lobe moves northward and becomes the main lobe. The time progression involves the entire interference pattern moving northward, appearing on the southern edge of the slab, and disappearing on the northern edge. We emphasize that this figure shows the HF power, not the ELF/VLF power, and there is no overall north/south disparity in the total power density injected into the ionosphere. Any north/south disparity in the ELF/VLF generated pattern on the ground therefore results from either the phasing of the HF power, or the anisotropy of the HF heating and cooling process.

[18] For the case shown in Figure 1, the northward HF source is lower in frequency, and the interference pattern moves northward. On the other hand, if the southward HF source were lower in frequency, the interference pattern moves southward. As such, we distinguish two types of beat wave techniques, in which the HF interference pattern can move to the north, or to the south, due to the spatial separation of the two HF sources. On the other hand, traditional amplitude modulation can be thought of as resulting from a single source. For amplitude modulation, the pattern looks like the top left panel of Figure 1, and the power simply modulates as a sinusoid in time, with no spatial motion.

[19] Figure 2 shows the calculated magnetic field on the ground for amplitude modulation, over a 250 km × 250 km box centered at HAARP. The power is assumed to be modulated sinusoidally in time. The propagation model yields all three components of the magnetic field, and the plotted value is the sum in quadrature of the two horizontal magnetic field components (the vertical component is negligible because of the high conductivity of the ground, and it is typically not recorded in ELF/VLF ground measurements). The 12 panels represent 12 different ELF/VLF frequencies, ranging from 1 kHz to 21.5 kHz, labeled in the top left corner of each panel. These correspond to the same 12 frequencies that were part of the experiment described by *Kuo et al.* [2012] that compared amplitude modulation to beat wave. The radiation pattern from sinusoidal power modulation is mostly isotropic around

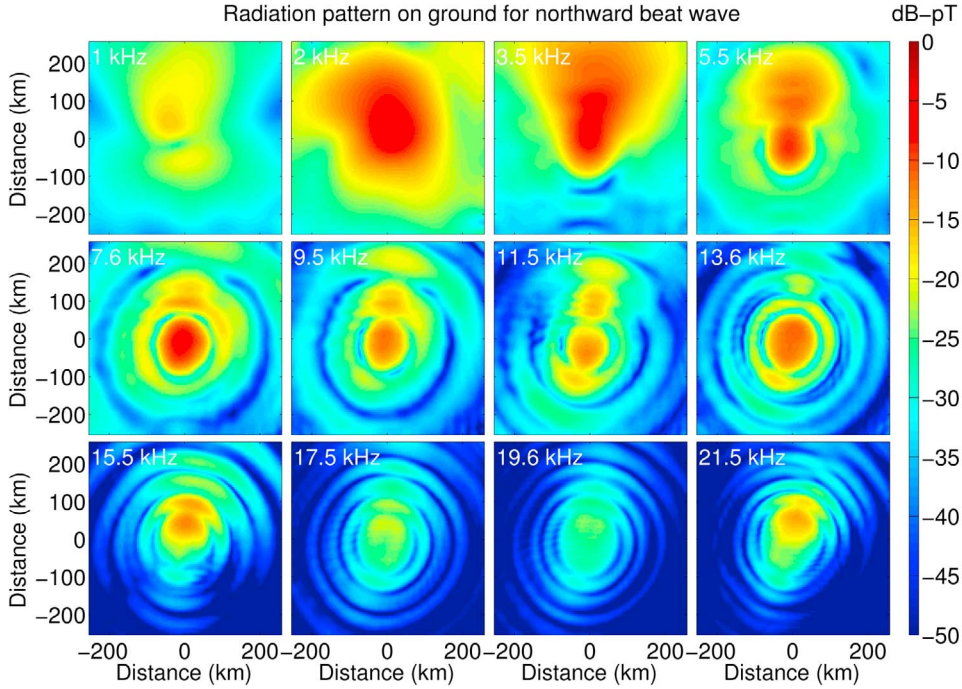

Figure 3. Same calculations as in Figure 2, except applied to the northward beat wave, where the northern half of HAARP operated at the lower HF frequency, and the HF radiation pattern thus moves northward.

HAARP. There is some feature (most noticeable at 2 kHz) that looks like a spiral pattern, resulting from the non-vertical component of the geomagnetic field, and the asymmetric response of the Hall and Pedersen conductivity, described in Figure 3 of *Cohen et al.* [2010a]. Also evident is the interference pattern of multimode ELF/VLF propagation, appearing as concentric rings around HAARP, particularly at the higher frequencies where more modes propagate, and the free space wavelength is shorter.

[20] Figures 3 and 4 show the calculated magnetic field for the northward and southward beat wave, with identical panels, and at the same set of 12 frequencies. The radiation pattern on the ground looks substantially different than the amplitude modulation results at all frequencies. The northward and southward beat wave radiation patterns also look essentially the same, but the directional dependence is reversed by 180°.

[21] A key effect in the directional pattern is the apparent physical horizontal speed of the HF heating pattern that enters the ionosphere. As the frequency of the beat wave separation increases, the HF power pattern moves to the north or south increasingly fast. As the speed of the beam approaches the phase velocity of propagating waves in the Earth-ionosphere waveguide, there is a traveling wave tube effect which acts to direct the radiation in a certain direction due to the matched propagation between the phase fronts of the generating ionospheric currents, and the phase fronts of the generated ELF/VLF wave. This effect is similar to the geometric modulation 'sawtooth sweep'. The HF radiation pattern moves horizontally at close to the speed of light at ~8 kHz [*Cohen et al.*, 2010b].

[22] Comparing Figures 3 and 4, this directional phasing effect is exhibited as a pronounced increase in radiated power in a northward (or southward) direction, observed most prominently between 3.5 and 9.5 kHz. Below 3.5 kHz, the motion is too slow, which limits the directional dependence of the radiation. Above 9.5 kHz, the HF radiation pattern moves faster than the speed of light, although nothing is carried faster than the speed of light, but rather the phase velocity of the interference pattern is faster than the speed of light. In addition to the directional phasing effect, some of the directional dependence arises from the asymmetric shape of the HF beam when it is comprised of a half-array, similar to the broadened east-west beam described by *Cohen et al.* [2012].

[23] Figure 5 shows the ratio of the ground magnetic field of northward beat wave to the ground magnetic field of amplitude modulation, on a logarithmic scale. Red areas indicate where the northward beat wave produces higher amplitude, blue indicates where amplitude modulation produces higher amplitude, white indicates similar magnetic field. There is a clear trend that with increasing frequency, the beat wave technique produces stronger magnetic fields compared to amplitude modulation. At 1 and 2 kHz, amplitude modulation produces stronger magnetic fields. At 3.5 kHz, northward beat wave is stronger to the north of HAARP, but amplitude modulation is stronger to the south of HAARP. Starting at 5.5 kHz, beat wave generation becomes increasingly advantageous compared to amplitude modulation, even in the southward direction from HAARP. Although not shown, a similar plot of the ratio of southward beat wave to amplitude modulation looks almost identical to Figure 5, except that the vertical axis is flipped. As noted earlier, square-wave amplitude modulation would produce ELF/VLF amplitudes that are 1–3 dB stronger than those produced using sinusoidal power modulation. An analysis using square-wave amplitude modulation would yield similar results as shown in Figure 5,

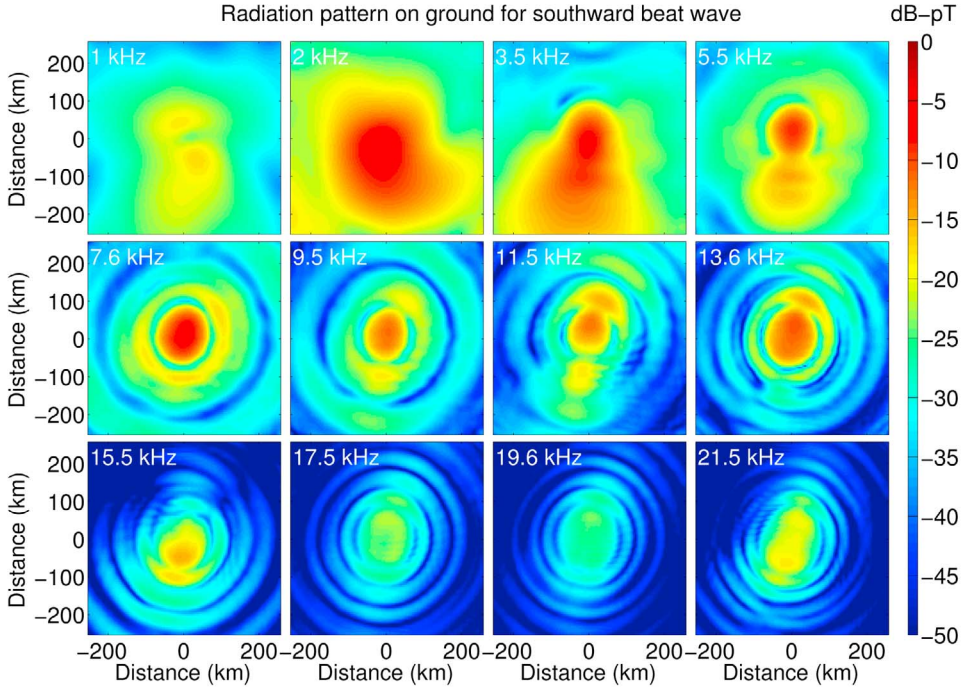

Figure 4. Same calculations as in Figure 2, except applied to the southward beat wave, where the southern half of HAARP operated at the lower HF frequency, and the HF radiation pattern thus moves southward.

except that the frequency at which beat-wave modulation becomes more efficient would be slightly higher.

[24] Figure 6 shows the calculated magnetic field at three locations, at HAARP (Figure 6, left), 150 km northward of HAARP (Figure 6, middle), and 150 km eastward of HAARP (Figure 6, right). As in the previous descriptions, 'north' refers to the direction along HAARPs north-south axis, which is 14° east of geographic north, and 8° west of geomagnetic north at HAARP. At HAARP, amplitude modulation has a frequency content that steadily decreases with increasing frequency beyond ~2 kHz, although there is some deviation from a straight line due to resonances in the Earth-

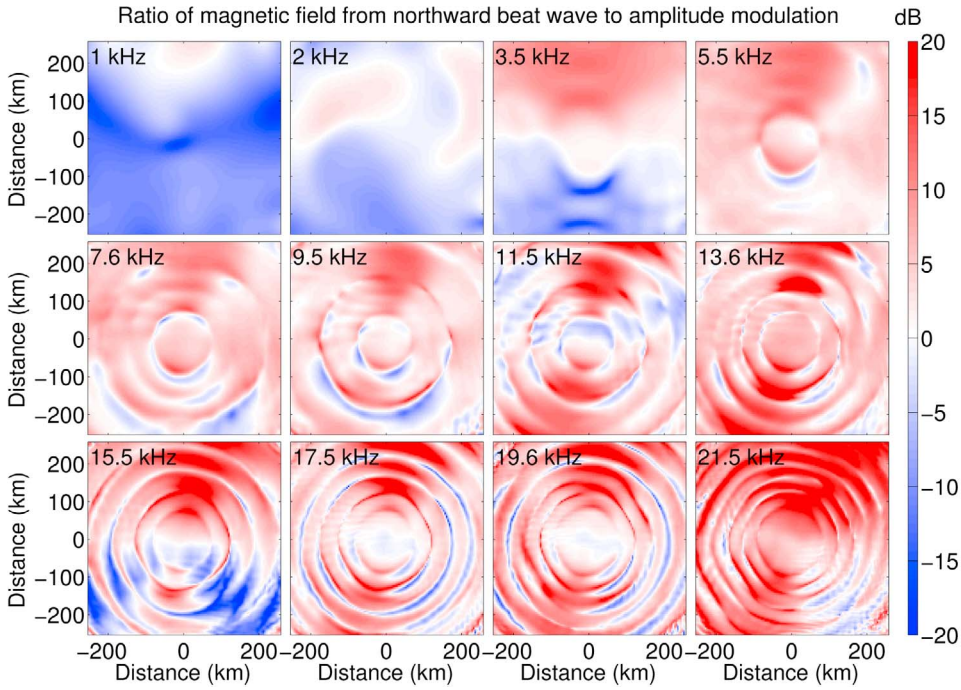

Figure 5. The ratio of the magnetic field on the ground from the northward beat wave, to that of amplitude modulation, as a function of distance, for the same 12 frequencies discussed earlier.

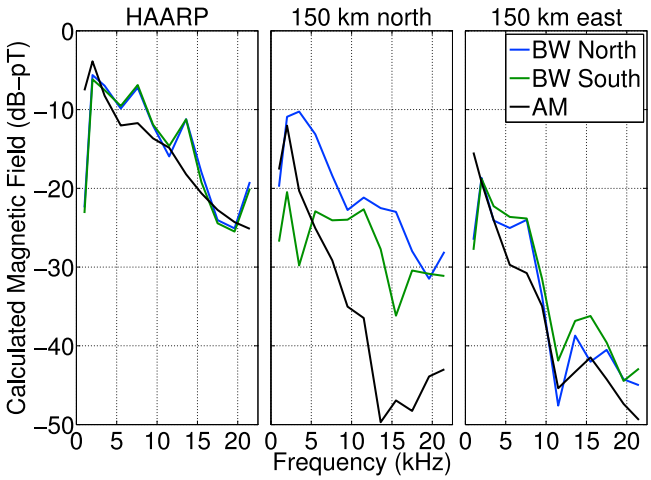

Figure 6. The total horizontal magnetic field predicted at three locations, including (left) directly at HAARP, (middle) 150 km along the northern axis of HAARP, and (right) 150 km to the east of HAARP.

ionosphere cavity [*Stubbe et al.*, 1982; *Rietveld et al.*, 1989; *Cohen et al.*, 2012]. The decrease in efficiency with frequency is not included in the model of *Barr and Stubbe* [1997], which assumed that ELF/VLF generation efficiency is proportional to HF power density and not to a function of ELF/VLF frequency. The model here includes the full heating and cooling physics and so the decrease in efficiency beyond 2 kHz present in all results of Figure 6 is a result of this effect. However, at most frequencies above 5 kHz, the northward and southward beat wave techniques produce stronger amplitudes than amplitude modulation, although they also seem to exhibit more variability with frequency.

[25] The two beat wave techniques are nearly identical at HAARP, due to the symmetry inherent from the fact that the receiver is right at the location of the array. However, the disparity between northward and southward beat waves is extremely strong 150 km north of HAARP, with a difference between the two as a high as 15 dB, similar to the geometric modulation sawtooth sweep [*Cohen et al.*, 2008b]. The north-south disparity is strongest between 3 and 10 kHz, corresponding to frequencies near where the speed of the radiation pattern entering the ionosphere is close to the speed of light. However, at a location 150 km to the east, the disparity between north and south beat wave techniques largely vanishes.

4. Discussion

[26] It should be emphasized that the model we describe here includes collisional absorption of HF heating and cooling only. At higher altitudes, >100 km, these effects disappear, as the atmosphere is thin and collisions too rare. Thus, ELF/VLF wave generation via this technique does not efficiently occur above 100 km, because the ionosphere recovers much more slowly than the 10 s to 100 s of μs periods in the ELF/VLF range. The theoretical formulation for whistler wave generation in the *F*-region [*Kuo et al.*, 2011, 2012], is thus not included in the model.

[27] Nonetheless, the model shows that beat wave generation can be a substantially more effective technique for ELF/VLF wave generation compared to amplitude modulation. We do note that the beat wave approach uses 3 dB more HF power since both halves of the array transmit at full power (whereas for amplitude modulation the average power is half the maximum), but even after accounting for this, beat wave generation yields up to 10–20 dB stronger signal amplitudes at some locations.

[28] We thus conclude that the beat wave method for ELF/VLF wave generation generally produce more ELF/VLF power than sinusoidal power modulation at frequencies above ~5 kHz, by virtue of the phasing effects of the signal generation in the D-region ionosphere. An F-region source is thus not needed to explain the results of *Kuo et al.* [2012], who present higher amplitudes for beat wave compared to amplitude modulation as evidence for an F-region source. Given that generation in the *D*-region has a long and well documented history, whereas *F*-region generation via beat wave has not been demonstrated prior to these recent papers, we conclude that an *F*-region source mechanism with beat wave HF heating remains unvalidated. While we cannot rule out the feasibility of the physical mechanism suggested by *Kuo et al.* [2011, 2012], it seems clear that further experiments are required to establish the viability of the electrojet-independent beat wave generation technique.

[29] **Acknowledgments.** This work has been supported by ONR award N0014-09-1-0100 and AFRL award FA9453-11-C-0011 to Stanford University with subaward 27239350-50917-B to CU Denver. This work is also supported by NSF grants AGS-0940248 and ANT-0944639, ONR grant N000141010909, DARPA contract HR0011-09-C-0099, and DARPA grant HR0011-10-1-0061 to University of Florida with subaward UF-EIES-1005017-UCD to CU Denver. The experiments were conducted as part of the SSRC summer campaign at HAARP, and we thank Ed Kennedy for organizing it. We thank Mike McCarrick and the HAARP operators for their help.

[30] Robert Lysak thanks the reviewers for their assistance in evaluating this paper.

References

Banks, P. (1966), Collision frequencies and energy transfer: Electrons, *Planet. Space Sci.*, *14*, 1085–1103.

Barr, R. (1998), The generation of ELF and VLF radio waves in the ionosphere using powerful HF transmitters, *Adv. Space Res.*, *21*(5), 677–687.

Barr, R., and P. Stubbe (1984), ELF and VLF radiation from the 'polar electrojet antenna,' *Radio Sci.*, *19*(4), 1111–1122.

Barr, R., and P. Stubbe (1991), ELF radiation from the Tromsø "super heater" facility, *Geophys. Res. Lett.*, *18*(6), 1035–1038.

Barr, R., and P. Stubbe (1997), ELF and VLF wave generation by HF heating: A comparison of AM and CW techniques, *J. Atmos. Sol. Terr. Phys.*, *18*(58), 2265–2279.

Barr, R., M. T. Rietveld, P. Stubbe, and H. Kopka (1987), Ionospheric heater beam scanning: A mobile source of ELF/VLF radiation, *Radio Sci.*, *22*(6), 1076–1083.

Bittencourt, J. (2003), *Fundamentals of Plasma Physics*, 3rd ed., Springer, New York.

Cohen, M. B., M. Gołkowski, and U. S. Inan (2008a), Orientation of the HAARP ELF ionospheric dipole and the auroral electrojet, *Geophys. Res. Lett.*, *35*, L02806, doi:10.1029/2007GL032424.

Cohen, M. B., U. S. Inan, and M. Gołkowski (2008b), Geometric modulation: A more effective method of steerable ELF/VLF wave generation with continuous HF heating of the lower ionosphere, *Geophys. Res. Lett.*, *35*, L12101, doi:10.1029/2008GL034061.

Cohen, M. B., U. S. Inan, M. Gołkowski, and N. G. Lehtinen (2010a), On the generation of ELF/VLF waves for long-distance propagation via steerable HF heating of the lower ionosphere, *J. Geophys. Res.*, *115*, A07322, doi:10.1029/2009JA015170.

Cohen, M. B., U. S. Inan, M. Gołkowski, and M. J. McCarrick (2010b), ELF/VLF wave generation via ionospheric HF heating: Experimental

comparison of amplitude modulation, beam painting, and geometric modulation, *J. Geophys. Res.*, *115*, A02302, doi:10.1029/2009JA014410.

Cohen, M. B., U. S. Inan, and E. P. Paschal (2010c), Sensitive broadband ELF/VLF radio reception with the AWESOME instrument, *IEEE Trans. Geosci. Remote Sens.*, *48*(1), 3–17, doi:10.1109/TGRS.2009.2028334.

Cohen, M. B., U. S. Inan, D. Piddyachiy, N. G. Lehtinen, and M. Golkowski (2011), Magnetospheric injection of ELF/VLF waves with steerable HF heating of the lower ionosphere, *J. Geophys. Res.*, *116*, A06308, doi:10.1029/2010JA016194.

Cohen, M. B., M. Golkowski, N. G. Lehtinen, U. S. Inan, and M. J. McCarrick (2012), HF beam parameters in ELF/VLF wave generation via modulated heating of the ionosphere, *J. Geophys. Res.*, *117*, A05327, doi:10.1029/2012JA017585.

Dalgarno, A., M. B. McElroy, M. H. Rees, and J. C. G. Walker (1968), The effect of oxygen cooling on ionsspheric electron temperatures, *Planet. Space Sci.*, *16*, 1371–1380.

Fujimaru, S., and R. C. Moore (2011), Analysis of time-of-arrival observations performed during ELF/VLF wave generation experiments at HAARP, *Radio Sci.*, *46*, RS0M03, doi:10.1029/2011RS004695.

Getmantsev, C. G., N. A. Zuikov, D. S. Kotik, N. A. Mironenko, V. O. Mityakov, Y. A. Rapoport, V. Y. Sazanov, V. Y. Trakhtengerts, and V. Y. Eidman (1974), Combination frequencies in the interaction between high-power short-wave radiation and ionsopheric plasma, *J. Exp. Theor. Phys.*, *20*, 101–102.

Golkowski, M., U. S. Inan, A. R. Gibby, and M. B. Cohen (2008), Magnetospheric amplification and emission triggering by ELF/VLF waves injected by the 3.6 MW HAARP ionospheric heater, *J. Geophys. Res.*, *113*, A10201, doi:10.1029/2008JA013157.

Golkowski, M., M. B. Cohen, D. L. Carpenter, and U. S. Inan (2011), On the occurrence of ground observations of ELF/VLF magnetospheric amplification induced by the HAARP facility, *J. Geophys. Res.*, *116*, A04208, doi:10.1029/2010JA016261.

Jin, G., M. Spasojevic, M. B. Cohen, U. S. Inan, and N. G. Lehtinen (2011), The relationship between geophysical conditions and ELF amplitude in modulated heating experiments at HAARP: Modeling and experimental results, *J. Geophys. Res.*, *116*, A07310, doi:10.1029/2011JA016664.

Kotik, D. S., L. F. Mironenko, S. N. Mityakov, V. O. Rapoport, V. A. Solynin, and V. V. Tamojkin (1986), On the possibility of the formation of a faster-than-light source of Cherenkov radiation due to the Getmantsev effect (in Russian), in *Modification of the Ionosphere by Powerful Radio Waves*, pp. 91–92, Suzdal, Moscow.

Kuo, S. P., A. Snyder, P. Kossey, C. L. Chang, and J. Labenski (2011), VLF wave generation by beating of two HF waves in the ionosphere, *Geophys. Res. Lett.*, *38*, L10608, doi:10.1029/2011GL047514.

Kuo, S. P., A. Snyder, P. Kossey, C. L. Chang, and J. Labenski (2012), Beating HF waves to generate VLF waves in the ionosphere, *J. Geophys. Res.*, *117*, A03318, doi:10.1029/2011JA017076.

Lehtinen, N. G., and U. S. Inan (2008), Radiation of ELF/VLF waves by harmonically varying currents into a stratified ionosphere with application to radiation by a modulated electrojet, *J. Geophys. Res.*, *113*, A06301, doi:10.1029/2007JA012911.

Lehtinen, N. G., and U. S. Inan (2009), Full-wave modeling of transionospheric propagation of VLF waves, *Geophys. Res. Lett.*, *36*, L03104, doi:10.1029/2008GL036535.

Lunnen, R. J., H. S. Lee, A. J. Ferraro, T. W. Collins, and R. F. Woodman (1984), Detection of radiation from a heated and modulated equatorial electrojet current system, *Nature*, *311*(13), 134–135.

Mentzoni, M. H., and R. V. Row (1963), Rotational excitation and electron relaxation in nitrogen, *Phys. Rev.*, *130*, 2312–2316.

Milikh, G. M., and K. Papadopoulos (2007), Enhanced ionospheric ELF/VLF generation efficiency by multiple timescale modulated heating, *Geophys. Res. Lett.*, *34*, L20804, doi:10.1029/2007GL031518.

Moore, R. C. (2007), ELF/VLF wave generation by modulated HF heating of the auroral electrojet, PhD thesis, Stanford Univ., Stanford, Calif.

Moore, R. C., and D. Agrawal (2011), ELF/VLF wave generation using simultaneous CW and modulated HF heating of the ionosphere, *J. Geophys. Res.*, *116*, A04217, doi:10.1029/2010JA015902.

Moore, R. C., U. S. Inan, T. F. Bell, and E. J. Kennedy (2007), ELF waves generated by modulated HF heating of the auroral electrojet and observed at a ground distance of ∼4400 km, *J. Geophys. Res.*, *112*, A05309, doi:10.1029/2006JA012063.

Moore, R. C., S. Fujimaru, M. B. Cohen, M. Golkowski, and M. McCarrick (2012), On the altitude of the ELF/VLF source region generated during beat-wave HF heating experiments, *Geophys. Res. Lett.*, *39*, L18101, doi:10.1029/2012GL053210.

Papadopoulos, K., N. A. Gumerov, X. M. Shao, I. Doxas, and C. L. Chang (2011), HF-driven currents in the polar ionosphere, *Geophys. Res. Lett.*, *38*, L12103, doi:10.1029/2011GL047368.

Payne, J. A., U. S. Inan, F. R. Foust, T. W. Chevalier, and T. F. Bell (2007), HF modulated ionospheric currents, *Geophys. Res. Lett.*, *34*, L23101, doi:10.1029/2007GL031724.

Rapoport, V. O., D. S. Kotik, L. F. Mironenko, and S. N. Mityakov (1994), Experimental study of low-frequency emission from a mobile ionospheric source, *Radiophys. Quantum Electron.*, *37*(6), 507–513.

Rietveld, M. T., R. Barr, H. Kopka, E. Nielsen, P. Stubbe, and R. L. Dowden (1984), Ionospheric heater beam scanning: A new technique for ELF studies of the auroral ionosphere, *Radio Sci.*, *19*(4), 1069–1077.

Rietveld, M. T., H. P. Mauelshagen, P. Stubbe, H. Kopka, and E. Nielsen (1987), The characteristics of ionospheric heating-produced ELF/VLF waves over 32 hours, *J. Geophys. Res.*, *92*(A8), 8707–8722.

Rietveld, M. T., P. Stubbe, and H. Kopka (1989), On the frequency dependence of ELF/VLF waves produced by modulated ionospheric heating, *Radio Sci.*, *24*(3), 270–278.

Rodriguez, J. V. (1994), Modification of the Earth's ionosphere by very low frequency transmitters, PhD thesis, Stanford Univ., Stanford, Calif.

Sen, H. K., and A. A. Wyller (1960), On the generalization of the Appleton-Hartree magnetoionic formulas, *J. Geophys. Res.*, *65*, 3931–3950.

Stubbe, P., and W. S. Varnum (1972), Electron energy transfer rates in the ionosphere, *Planet. Space Sci.*, *20*, 1121–1126.

Stubbe, P., H. Kopka, and R. L. Dowden (1981), Generation of ELF and VLF waves by polar electrojet modulation: Experimental results, *J. Geophys. Res.*, *86*(A11), 9073–9078.

Stubbe, P. H., H. Kopka, M. T. Rietveld, and R. L. Dowden (1982), ELF and VLF generation by modulated heating of the current carrying ionosphere, *J. Atmos. Terr. Phys.*, *44*(12), 1123–1135.

Tomko, A. A. (1981), Nonlinear phenomena arising from radio wave heating of the lower ionosphere, Ph.D. thesis, Pa. State Univ., University Park.

Villaseñor, J., A. Y. Wong, B. Song, J. Pau, M. McCarrick, and D. Sentman (1996), Comparison of ELF/VLF generation modes in the ionosphere by the HIPAS heater array, *Radio Sci.*, *31*(1), 211–226.

Watt, A. D. (1967), *VLF Radio Engineering*, Pergamon, New York.